Facile Synthesis of Nanostructured Dentritic Polythiophene Nickel Composite and Its Application in the Adsorptive Removal of Methylene Blue

Abhishek Kumar Mishra[a,b], Ishwar Das[a] and Namita Rani Agrawal[b*]
[a] Chemistry Department, D.D.U. Gorakhpur University, Gorakhpur, India
[b] Chemistry Department, St. Andrew's College Gorakhpur, India

ABSTRACT

Polythiophene nickel nanocomposite was electrochemically synthesized from solution containing thiophene, perchloric acid and nickel chloride in acetonitrile medium and its application as adsorbent for the removal of Methylene blue (MB) dye was investigated. Polythiophene nickel composite (PTh-Ni composite), showed excellent water dispersibility. Polymer aggregates were characterized by transmission electron microscopy (TEM), Powder X-ray diffraction (XRD), Fourier Transform Infrared Spectroscopy (FT-IR), electrical conductivity and fractal dimension calculation. Electrical conductivity was found to increase with increase in nickel chloride concentration. Particles of the polythiophenes nickel composite were showed average size < 5 nm. Optimum dosage of adsorbent were determined and found to be1.5 gL^{-1} for PTh-Ni composite. Adsorption capacity (Q) is found to increase with increase in pH values. Experimental data were tested using Langmuir, Frendlich and Temkin models, and data were best followed by Freundlich model at 30°C. The maximum adsorption capacity (Q$_m$) for PTh-Ni composite was found to be 384.61 mg/g. Various kinetic equations were applied to kinetic data and were best followed by pseudo-second-order kinetic model. The thermodynamic parameters such as change in enthalpy ($\Delta H°$), entropy ($\Delta S°$), and free energy ($\Delta G°$) were calculated. The adsorption is spontaneous and endothermic in nature. Adsorption/desorption results are also reported.

Keywords: Nanostructure, Conducting polymer, Adsorption, Methylene blue, PTh-Ni composite.

I. INTRODUCTION

Dyes are one of the most easily recognizable environmental pollutants. Various industries such as textile, leather, cosmetic, paper, printing, plastics, rubber, pharmaceutical and food are the sources of pollutant dyes since they all use it in their products [1]. Discharging of dyes into water resources even in a small amount can affect the aquatic life and food web. Dye can also cause allergic dermatitis and skin irritation. Some of them have been reported to be carcinogenic and mutagenic for aquatic organism and humans [2]. Methylene blue in particular, can cause some specific harmful effect in the human body such as heart beat increase, shockes and cyanosis [3].

Various physic-chemical methods are used for removal of dyes, such as membrane filtration, adsorption, chemical oxidation, coagulation/flocculation, ion exchange, reverse osmosis and precipitation. In those superior methods, the adsorption has been considered as a favorable procedure due to economic feasibility; recycle of adsorbent and nonexistence of harmful residues [4].

Conducting polymers such as polythiophene with large π-conjugated structure have received considerable attention due to their potential applications in chemical and biological sensors, rechargeable batteries, light emitting diodes, corrosion resistance [5-7], electrochemical capacitors [8] etc. But recent advances have been made in the application of conductive polymers and their derivatives for water purification applications, targeting various pollutants such as heavy metals [9], harmful microorganisms [10], and various industrial dyes [11, 12].

In the present chapter we have synthesized dendritic polythiophene nickel nanocomposite (PTh-Ni composite) by electrochemical method at room temperature and used as an effective adsorbent for removal of methylene blue from its aqueous solution. Its characterization done by FT-IR, XRD, TEM, fractal dimension (D) and electrical conductivity measurements. Influence of nickel chloride concentrations and field intensities on the morphology and growth kinetics will be investigated. Adsorption capacity (Q) of PTh-Ni composite will be investigated for removal of MB from its aqueous solution. The adsorption of MB onto polymer aggregates, effect of initial solution concentration, contact time, pH and temperature will be systematically investigated. Kinetics and adsorption isotherms for the adsorption of MB on to PTh-Ni composite will be studied. Desorption and repeatability studies are also carried out.

II. METHODS AND MATERIAL

Thiophene (Spectrochem Pvt. Ltd., Mumbai, India), Perchloric acid 70% (AR, s. d. fine chem. Ltd., Mumbai, India), nickel chloride (Qualigens Pvt. Ltd., Bombay, India, AR), acetonitrile (s. d. fine chem. Ltd., LR, Mumbai, India), Methylene blue (Qualigens fine chemicals) and milli-Q water were used as such.

1. Synthesis of polythiophene nickel composite

Polythiophene nickel composite was electrochemically synthesized by anodic oxidation of thiophene in acetonitrile medium containing perchloric acid and nickel chloride under potentiostatic condition using an experimental set-up described earlier [13]. 10 mL of a solution containing thiophene, perchloric acid, nickel chloride and acetonitrile in an appropriate proportion was taken in petri dish. Cleaned platinum vertical anode (diameter 0.4mm) and a circular platinum cathode were employed. The vertical anode was put at the centre of circular cathode such as to touch the air / liquid interface. These electrodes were attached to a potentiostat (Scientific India). Polymerization started at the anode as soon as the potential was applied across the electrodes. The aggregates were washed properly and dried. Patterns were photographed using a Nikon camera. Morphologies of polythiophene nickel composite aggregates obtained at different concentration of nickel chloride are shown in Table 1.

The time of electropolymerization was 30 min. in each case.

Growth kinetics was studied by recording weight of polymer aggregates at different time, concentrations of nickel chloride and field intensity. Results are shown in Fig. 1.

2. Characterization

Fractal dimension (D) of growth patterns of polythiophene nickel chloride was calculated by box counting method as described earlier [14]. Results are recorded in Table 1. The electrical conductivity of solid polymer aggregates was measured as described earlier [15]. Results are shown in Fig. 2. XRD studies of polythiophene and polythiophene nickel composite were carried out at Central Salt and Marine Chemical Research Institute, Bhavnagar, Gujarat, India. Result is shown in Fig. 3. FT-IR spectra of polythiophene and polythiophnene nickel composite were taken using a spectrophotometer model Thermo Nicolet, Avatar 370 and shown in Fig. 4. TEM images of PTh-Ni composite were taken using a Philips Transmission Electron Microscope (Model CM 200). Results are shown in Fig. 5.

3. Adsorption experiments

Methylene blue (MB) solutions of different concentrations in the range 100- 600 mgL^{-1} were prepared to obtain a calibration curve to verify Lambert-Beer Law. Absorbance of each solution of MB was measured at λ_{max} 664 nm as reported earlier [16]. To obtain optimum adsorbent dosage adsorption experiments were carried out by adding different amount of electrochemically synthesized powdered polythiophene nickel composite (0.5- 3.0 gL^{-1}), into 10 mL of an aqueous solution of MB (600 mgL^{-1}) in a small conical flask fitted with stopper. The solution was stirred vigorously for 60 minutes. The adsorbent was then separated out from the solution by centrifugation technique. Absorbance of the supernatant liquid was measured at 664 nm using a Double Beam microprocessor UV – Vis. Spectrophotometer [Model: LI – 2802]. Result for the removal % of MB for different amount of adsorbent dosages and corresponding adsorption capacity (Q) are shown in Fig. 6 At the optimum adsorbent dosage (1.5gL^{-1}) experiment was performed to measure adsorption

capacity (Q_t) of the adsorbent (PTh-Ni composite) at different contact time (5- 60 min) with different initial concentration of MB (100- 600 mgL^{-1}). Results are shown in Fig. 7 Studies of adsorption kinetics and adsorption isotherms are also done and results are shown in Figs. 8 (Table 2) and 9 (Table 3) respectively. Experiment was also performed to measure adsorption capacity (Q) for adsorbent at temperature 30, 40, 50 and 60 °C in an incubator at initial concentration 600 mgL^{-1} of MB for contact time 60 min. Results are shown in Fig. 11. The thermodynamic data are recorded in Table 4. The effect of pH on adsorption capacity (Q) value of adsorbent was studied at the dye concentration 600 mgL^{-1} at room temperature and pH values in the range 2- 10. Results are shown in Fig. 10 pH was measured using digital pH meter (Remi).

4. Desorption and repeatability studies

The desorption study was carried out by taking 15 mg of the adsorbent in10 mL aqueous of MB solution (600 mgL^{-1}) in a small conical flask fitted with stopper and the mixture was shaken on a magnetic stirrer at 150 rpm for 60 min. The MB-adsorbed adsorbent was then separated out from MB solution by centrifuging and added into 10 mL of methanol for desorption process and stirred for 60 min, the adsorbent was separated out from methanol, this desorption process was repeated 5 times. Then the adsorbent was collected by centrifugation technique and reused for adsorption again. The supernatant solution was analyzed by UV-Vis spectra. This adsorption and desorption cycle were successively carried out four times for the adsorbent used in this study.

Desorption and repeatability experiment was carried out in duplicate for adsorbent and average values of adsorption capacity are recorded. Adsorption capacity (Q) of adsorbent at different adsorption cycles are shown in Fig. 12.

5. Chi-Square ($\chi 2$) Test

Chi-square ($\chi 2$) statistical test was carried out by using equation (1) [17].

$$\chi 2 = \frac{\sum_{i=1}^{n}(Q_{e,cal} - Q_{e,exp})_i^2}{Q_{e,exp}} \quad \text{----------- (1)}$$

where $Q_{e,cal}$ and $Q_{e,exp}$ are calculated and experimental data respectively. The magnitude of $\chi 2$ was used to determine the closeness of the calculated model data to the experimental data.

III. RESULTS AND DISCUSSION

## 1. Characterization of polythiophene nickel composite

Polythiophene nickel composite aggregates were produced via electropolymerization using different time (min), concentrations of nickel chloride (M) and field intensities (V/cm). Results are shown in Fig. 1. Weight of polythiophene nickel composite was measured at different time, keeping other parameters fixed and found increases non- linearly. Result is shown in Fig. 1(a). When the experiment was carried out at different nickel chloride concentrations, weight of the polymer aggregate was found to decreases non linearly as shown in Fig. 1(b). Critical field intensity at 3.6 V/cm was observed beyond which weight of the polymer aggregates decreased as shown in Fig. 1(c). At high anodic potential large current flows through the system may lead to loss of π- conjugation and degradation of polymer [18].
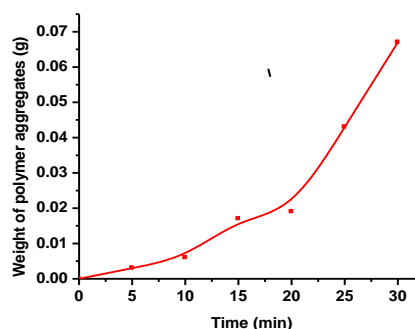

(a)
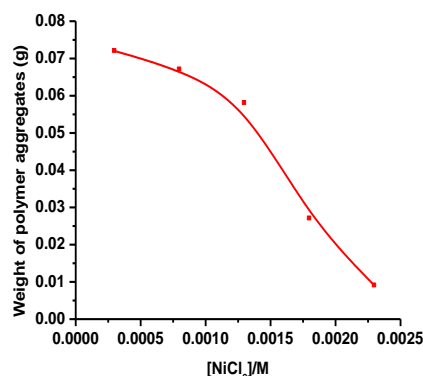
(b)
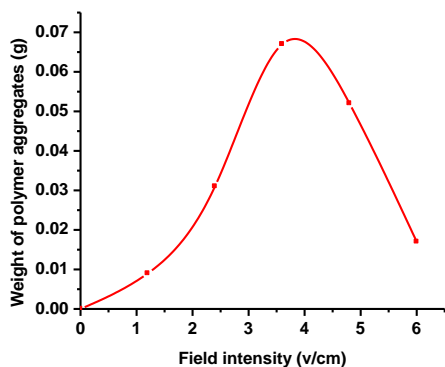
(c)

Figure 1. Plots showing weight of PTh-Ni Composite at different (a) time of polymerization (5, 10, 15, 20, 25, 30 min), (b) concentrations of nickel chloride (0.0003-0.0023 M) and (c) field intensities (1.2, 2.4, 3.6, 4.8 and 6.0 v/cm).

In the presence of electric field, oxidation of monomer takes place at the surface of the electrode to form the radical cation which is further stabilized by resonance. The next step involves radical cation coupling. The radical cation having greater unpaired electron density at α position reacts with other radical cation of the monomer to form a dimer. The dimer obtained during the electropolymerization was further oxidized to the dimer radical cation with greater electron density at α position. It reacts with the other radical cation of monomer to form a trimer. The process is repeated again and again resulting in the formation of polymer. The electropolymerization gives the neutral conductive polymer by doping of anions (Cl^-, ClO_4^-). In addition to $\alpha - \alpha'$ linkage in polythiophene, some $\alpha - \beta$ linkage can also take place similar to polypyrrole [18]. It can lead to greater random motion of radical cation leading to the formation of complex dendritic patterns [19].

$(x^- = ClO_4^-, Cl^-)$
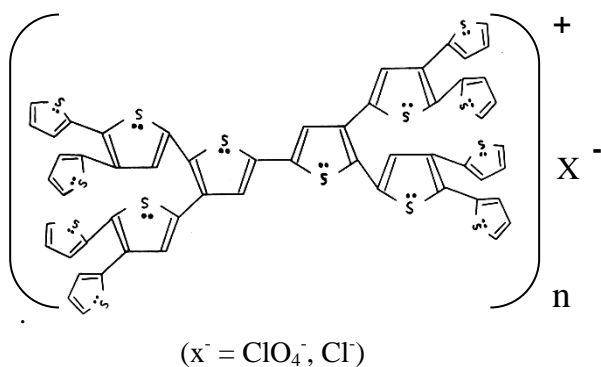
Polythiophene composite was electrodeposited from a solution containing thiophene, nickel chloride as the source of metal ion. During this process the nickel metal ion is encapsulated in polythiophene matrix as reported for encapsulation of metal ion in dendrimers [19, 20].

Electrical conductivity (σ) was measured in the solid state and found to increase linearly with concentration of Ni^{2+} (Fig. 2) obeying an empirical equation $\sigma = m[Ni^{2+}] + c$ where m and c are slope and intercept respectively. The correlation coefficient value was found to be 0.997. Similar trend was also observed by Zhu *et al* [21] for conducting polymetallorotaxanes while electrochemical inclusion of Cu^{2+} in the composite was reported by Gourier *et al* [22].
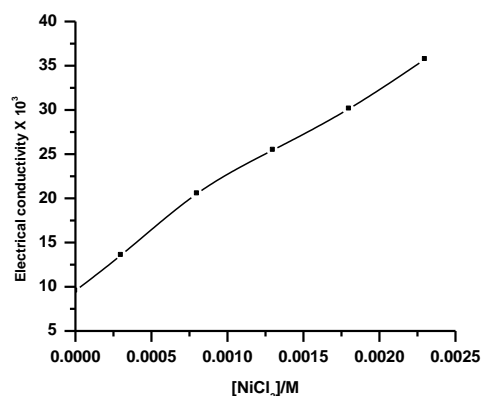

Figure 2. Electrical conductivity of Polythiophene nickel composite (PTh-Ni composite)

Fractal dimension of polymer aggregates of polythiophene nickel chloride were calculated by box counting method. The total number of pixels N(r) of radius r is related by the relationship $N(r) \sim r^D$. The fractal dimension (*D*) was calculated for images obtained at different nickel chloride concentrations from the plots of log N(r) versus log r. Results are recorded in Table 1. The values of *D* lie in the range 1.7- 1.8 in agreement with the value of Diffusion Limited Aggregation (DLA) model.

Table 1 . Values of fractal dimension *D* of 2-D views of PTh-Ni composites. Field intensity = 1.2 V/cm.

—

| [NiCl₂]/M	Fractal Dimension (D)	Morphology
0.0003	1.70	
0.0008	1.72	
0.0013	1.75	
0.0018	1.79	
0.0023	1.80	

XRD patterns of polythiophene and polythiophene nickel chloride are shown in Fig 3. The polythiophene (PTh) shows a broad peak around 24° as reported earlier which get shifted around 25° for polythiophene nickel composite. It indicates the intermolecular $\pi - \pi$ stacking structure and amorphous packing of prepared polythiophene and its nickel composite [23- 24].
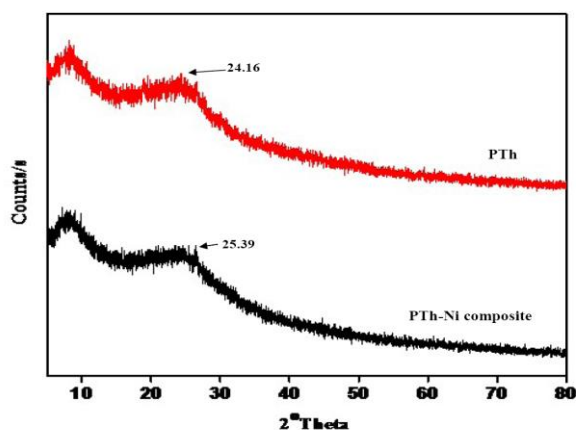
Figure 3. Powder X- ray diffraction for polythiophene (PTh) and polythiophene nickel composite (PTh-Ni composite). Conditions: [Th]= 1.5M, [HClO₄]= 0.1M, [Nickel chloride]= 0.0008M, Field intensity = 1.2 V/cm, Time of polymerization = 30 min.

The FT-IR spectrum of polythiophene (PTh) (Fig. 4) showed peaks at 2357 cm⁻¹, 1635 cm⁻¹, 1319 cm⁻¹, 1089 cm⁻¹, 787 cm⁻¹ and 623 cm⁻¹. The strong peak around 2357 cm⁻¹ is due to S – H stretch. The peak at 1635 cm⁻¹ represent asymmetric ring stretching contribution from –C=C- and –C-C- of the thiophene rings in polythiophene. The peak at 1319 cm⁻¹ is due to the ring breathing. The peaks present at 1089 cm⁻¹ are due to C-H in plane deformation. The peak present at 787 cm⁻¹ and 623 cm⁻¹ are due to the C-S stretching and C-H out of the plane deformation respectively. The bands situated at about 3389, 2357, 1635, 1319, 1089, and 787 cm⁻¹ in spectrum of polythiophene (PTh) were shifted to 3375, 2364, 1654, 1326, 1096, and 793 cm⁻¹ in spectrum of polythiophene nickel composite (PTh-Ni composite) conformed the interaction between nickel to thiophene ring of polythiophene [25- 26].
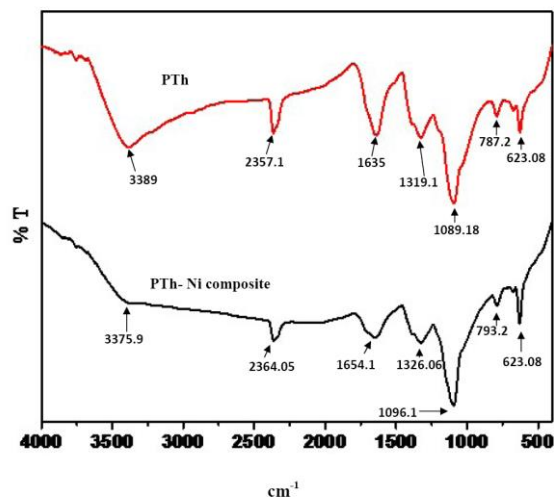
Figure 4. FT-IR spectra of polythiophene (PTh) and polythiophene nickel composite (PTh-Ni composite). Conditions: [Th] = 1.5M, [HClO₄] = 0.1M, [Nickel chloride] = 0.0008M, Field intensity = 1.2 V/cm, Time of polymerization = 30 min.

TEM images of are shown in Fig. 5. Spherical particles with an average diameter < 5 nm were observed for polythiophene nickel composite. Generally the size of the adsorbents at nanometer scale can result in a relatively large specific surface area, benefiting the sufficient contact between adsorbent and adsorbate [27]. Therefore, the electrochemically synthesized polythiophene nickel composite have potential application for the removal of organic dye (Methylene blue) from polluted water.
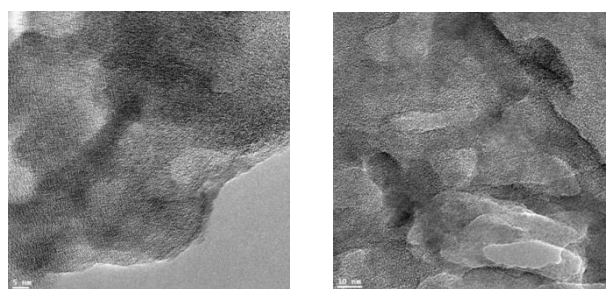
Figure 5. TEM images of Polythiophene nickel composite (PTh-Ni composite).

2. Adsorption studies

2.1. Determination of optimum adsorbent dosage

Optimum adsorbent dosage of electropolymerized polythiophene nickel composite was determined by taking different amount of adsorbent (0.5- 3.0 gL^{-1}) is mixed with MB solution of initial concentration 600 mgL^{-1} in a small conical flask fitted with stopper and stirred vigorously for a fixed period (60 minutes) at room temperature and centrifuged, the supernatant liquids were taken out for study of adsorption of MB. We observed that Absorbance was measured and found to be reduced due to the removal of MB from its aqueous solution was calculated by using equation (2)

$$\text{Removal \%} = \frac{C_O - C_e}{C_O} \times 100 \quad \text{------- (2)}$$

where C_o and C_e are the initial and MB concentration (mgL^{-1}) at equilibrium respectively. Results for removal % of MB for different adsorbents at different adsorbents dosages are shown in Fig. 6 (a). It shows that removal % of MB increases sharply upto adsorbent dosage 1.5 gL^{-1} and then increases gradually. It is also evident that polythiophene nickel composite (PTh-Ni composite) shows removal % of MB upto 95.7%. The adsorption capacity at equilibrium (Q_e) is an important indicator to evaluate the performance of the adsorbent which can calculate by using equation (3) [27- 28].

$$Q_e = \frac{(C_0 - C_e)V}{m} \quad \text{----------- (3)}$$

where V is the volume (L) of the MB solution, and m is the mass (g) of the adsorbent used. Adsorption capacity (Q_e) for adsorbent dosages are shown in Fig. 6(b). Results show that optimum adsorbent dosage for the adsorbent was found to be 1.5 gL^{-1} with highest adsorption capacity. At the optimum adsorbent dosage (1.5 gL^{-1}), adsorption capacity for adsorbent (PTh-Ni composite) is 334.4 mg/g.
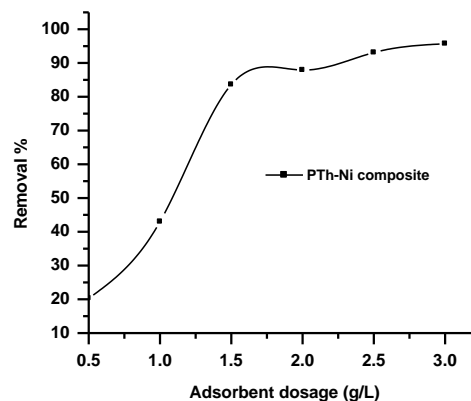
(a)
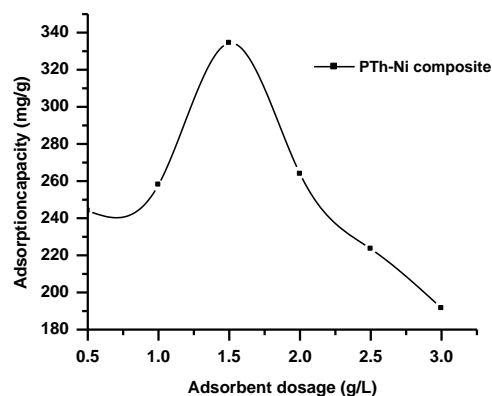
(b)

Figure 6. (a) Plots of Removal % MB at different adsorbent dosages (g/L); (b) Plots showing adsorption capacity (Q) at different adsorbent dosage (gL^{-1}) of Polythiophene nickel composite (PTh-Ni composite). Conditions: initial concentration of MB 600 mg/L; volume of MB solution = 10 mL; Contact time 60 min; temperature= 25°C; Oscillator speed = 150 rpm; at neutral pH.

2.2. Effect of initial MB concentration and contact time on adsorption capacity

The effect of contact time on the adsorption capacity (Q_t) for adsorbent studied for the removal of MB at different initial MB concentrations (100, 300 and 600 mgL^{-1}). The adsorption capacity (Q_t) at any time (t) was calculated by using equation (4) [27- 28].

$$Q_t = \frac{(C_0 - C_t)V}{m} \quad \text{----------- (4)}$$

Results are shown in Fig. 7 for adsorbent. The adsorption capacity increase sharply upto 20 min and attained equilibrium after 60 min in each case. It is also evident from this Figure the adsorption capacity increased with increase in the initial MB concentration indicating the strong interaction between adsorbents and

MB. The adsorption rate was fast in the first stage owning a large number of adsorption sites and the high concentration gradient of MB. As the adsorption carried on, equilibrium in adsorption capacity may be attended due to the saturation of the adsorption sites at higher MB concentrations. A similar tendency is reported for another adsorbent by other authors [30].
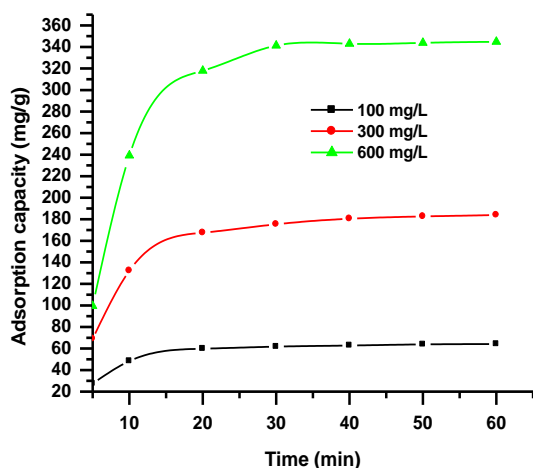
Figure 7. Effect of Contact time on adsorption capacity (Q_t) at different MB concentrations for PTh-Ni Composite. Conditions: volume of MB solution= 10 mL at neutral pH; temperature 25°C; adsorbent dosage 1.5 g/L; oscillator speed 150.

2.3. Adsorption kinetics

Adsorption kinetic provides information on the rate and mechanism of the adsorption. Adsorption kinetics has been studied using the results shown in Fig. 8 by using equations (5- 7) [31- 33]

$$\log (Q_e\text{-}Q_t) = \log Q_e - \frac{k_1 t}{2.303} \quad \text{-----------(5)}$$

$$\frac{t}{Q_t} = \frac{1}{k_2 Q_e^2} + \frac{1}{Q_e}\, t \quad \text{----------- (6)}$$

$$Q_t = \frac{1}{\beta} ln t + \frac{1}{\beta} \ln(\alpha\beta) \quad \text{------------ (7)}$$

where Q_t (mgg^{-1}) and Q_e (mgg^{-1}) are the amounts of MB adsorbed at any time and at equilibrium, respectively. k_1 (min^{-1}), k_2 (g mg^{-1} min^{-1}), α(mg g^{-1} min^{-1}) and β (g mg^{-1}) are the pseudo-first-order, pseudo-second-order model, initial adsorption rate and adsorption constants, respectively.
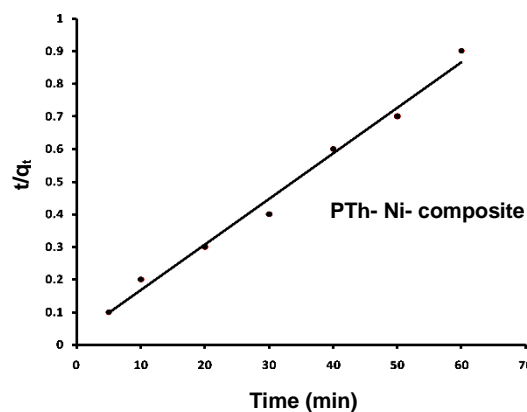
Figure 8. Linear fitting of kinetic plot: Pseudo-second-order kinetic model (T= 30°C; adsorbent dosage = 1.5 g L^{-1}; C$_0$ = 100 mg/L; shaking speed = 150 rpm).

The kinetic data were fitted with the pseudo- first-order, pseudo- second- order and Elovich models to describe kinetic characteristic of the adsorption of MB onto the polythiophene nickel composite. The relevant parameters for pseudo- first- order kinetics, pseudo-second – order kinetics and Elovich model are presented in Table 2. The values of Q_e for pseudo-first and pseudo-second-order kinetics were calculated and compared with experimental values as mentioned in Table 2. The calculated value of Q_e for pseudo-second-order kinetic was very close to the experimental value. The highest R^2 (0.989) and lowest $\chi 2$ (0.09) values suggested that the adsorption process was well described by the pseudo – second-order model. This suggests that the adsorption process is well described by the pseudo – second-order model. Based on the pseudo – second-order kinetic model, the chemical adsorption is found to be the rate-determining step which controls the process of adsorption of MB on polymer [34] which may involve electron sharing or electron transfer in the adsorption process between polymer and adsorbate [35].

Table 2. Kinetic parameters obtained from the pseudo-first-order, pseudo-second-order and Elovich models of MB adsorption on the PTh-Ni Composite (initial concentration of MB, 100 mg/L; volume, 10 mL; Contact time, 5, 10, 20, 30, 40, 50, 60 min; temperature, 25°C; adsorbent dosage, 1.5 g/L; oscillator speed, 150 rpm)

Kinetic models	Parameters	PTh- Ni composite
Pseudo-first-order	K	0.071
	Q_e(exp)	0.250
	Q_e(cal)	64.13
	R^2	0.819
	χ^2	1.08
Pseudo-second-order	K	0.0086
	Q_e(exp)	71.42
	Q_e(cal)	64.13
	R^2	0.989
	χ^2	0.09
Elovich	α	2.065
	β	0.072
	R^2	0.871
	χ^2	2.14

(a) — Langmuir plot: C_e/Q_e vs C_e (mg); $y = 0.0023x + 0.0682$, $R^2 = 0.9612$

(b) — Freundlich plot: $\log Q_e$ vs $\log C_e$; $y = 0.4852x + 1.5664$, $R^2 = 0.9911$

(c) — Temkin plot: $\ln C_e$ vs Q_e; $y = 0.0108x + 0.9908$, $R^2 = 0.9486$
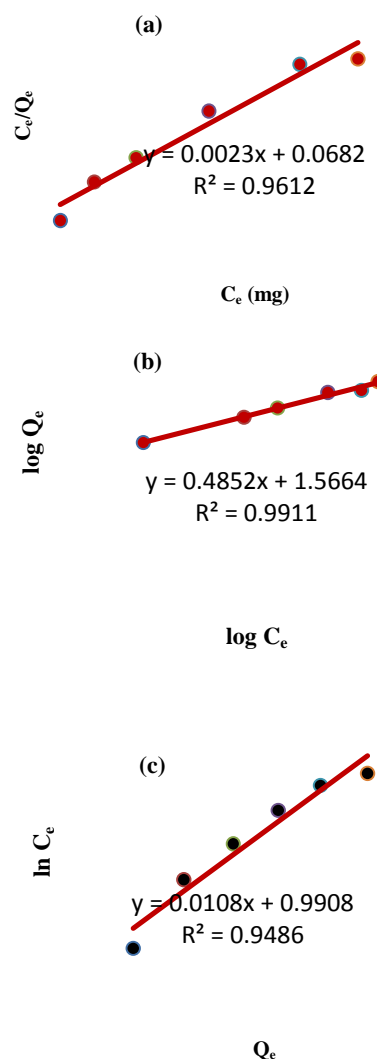
2.4. Adsorption isotherms

Equilibrium adsorption isotherms provides information about the relationship between the concentration of a dye in solution and the amount of dye adsorbed on the solid phase when both phases are in equilibrium, the isotherm data were fitted to Langmuir, Freundlich and Temkin models (Fig. 9). These three models are expressed in linear form by Equations (8- 10), respectively as employed earlier for other systems [31-33].

$$\frac{C_e}{Q_e} = \frac{1}{k_l Q_{max}} + \frac{C_e}{Q_{max}} \quad \text{----------- (8)}$$

$$\log Q_e = \log K_F + \frac{1}{n}\log C_e \quad \text{----------- (9)}$$

$$Q_e = B\ln A + B\ln C_e \quad \text{----------- (10)}$$

where K_L (L mg^{-1}) is the Langmuir constant, which is related to adsorption and maximum adsorption capacity, Q_{max} (mg g^{-1}) corresponding to complete monolayer coverage. K_F (mg$^{1-1/n}$ L$^{1/n}$ g^{-1}) is related to the adsorption capacity of the adsorbent and 1/n is a constant that is related to the adsorption intensity, A is the equilibrium constant of binding corresponding to the maximum energy of binding (mgL^{-1}) and the constant B is related to the heat of adsorption (Lmg^{-1}).

Figure 9. Linear fitting of adsorption isotherm plots: Langmuir model (a) Freundlich model (b) and Temkin model (c) for PTh-Ni composite (T= 30℃; adsorbent dosage = 1.5 g L^{-1}; C_0 = 100, 200, 300, 400, 500, and 600 mg/L; Contact time, 60 min; shaking speed = 150 rpm).

Different parameters based on Langmuir, Freundlich and Temkin models were calculated at 30 ℃ for different adsorbents and results are recorded in Table 3. The Correlation Coefficient values (R^2) for Freundlich isotherm model are very close to 1 for adsorbent. According to R^2 value of adsorption isotherm, the Freundlich model is more appropriate than the Langmuir and Temkin models for describing the adsorption behaviour of MB onto polymer. The essential characteristics of the Freundlich isotherm model can be expressed by parameters K_F and 1/n. If the 1/n value equals about 0.1-0.5, it means the adsorption process is easy to achieve (Table 3), indicating favorable adsorption of MB onto polymer. The value of

Q_m for PTh-Ni composite is found to be 384.6 mgg⁻¹. The value of K_L for PTh-Ni composite is given in Table 3. Temkin's isotherm considers the effect of heat of adsorption that decreases linearly with coverage of the adsorbate and adsorbent interaction. The linear plots of Q_e versus $\ln C_e$ enable to determine the constants A and B. The value of binding constant A and B is given in the Table 3. Therefore it can be used as promising adsorbent for the treatment of water waste that contains MB dye.

Table 3. Adsorption equilibrium parameters acquired from Langmuir, Freundlich and Temkin models in the adsorption of MB onto PTh-Ni Composite (initial concentration of MB, 100, 200, 300, 400, 500, and 600 mg/L; volume, 10 mL; Contact time, 60 min; temperature, 25°C; adsorbent dosage, 1.5 g/L; oscillator speed, 150 rpm)

Adsorption Isotherm Model	Parameters	Values
Langmuir model	Q_m K_L R^2	384.6 0.038 0.960
Freundlich model	$1/n$ n K_F R^2	0.4 2.0 36.98 0.990
Temkin model	A B R^2	1.0 0.010 0.948

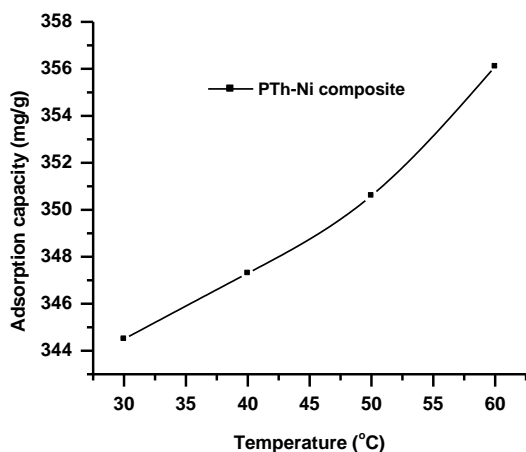## 2.5. Effect of initial pH of MB solution

The effect of pH values of MB solution on the adsorption capacity of the samples has been studied. Results are shown in Fig. 10. The experiments were performed using 600 mgL⁻¹ of initial MB concentration with the pH values in the range 2-10. Results show that adsorption capacity is low in the acidic medium. It is due to the competition of hydrogen ion with the cationic MB and the repulsive force between MB and positively charged adsorbents [36]. Further, the adsorption capacity was found to be higher in basic medium. Thus all the polymer samples studied may be used as efficient adsorbents at higher pH values.
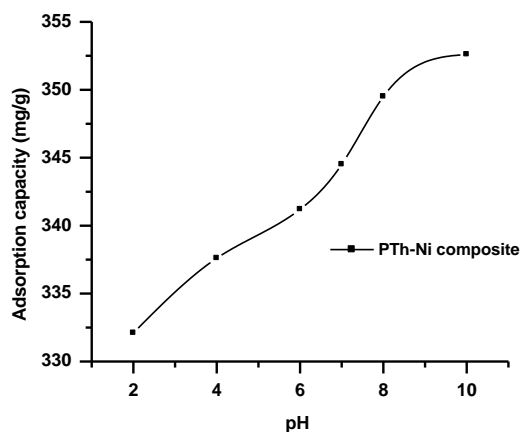
Figure 10. Effect of pH on adsorption capacity of MB solution onto PTh-Ni Composite. Conditions: initial concentration of MB= 600 mg/L; volume of MB solution = 10 mL; Contact time 60 min; temperature 25°C; adsorbent dosage 1.5 g/L; oscillator speed 150 rpm.

2.6. Effect of temperature and thermodynamic analyses

The effect of temperature on the adsorption capacity of MB for polythiophene nickel composite is shown in Fig. 11. Measurements were performed using 15 mg of adsorbent in 10 mL of 600mgL⁻¹ of MB at different temperatures (30, 40, 50, and 60°C) with contact time of 60 min. The adsorption capacity (Q_e) for MB removal is found to increase with increasing temperature indicating that the adsorption of MB on the adsorbents is favored at higher temperatures. This phenomenon may be attributed to the fact that polythiophene nickel composite result in the formation of closely packed polymer aggregates. There could be pores/ constrictions of size nearly equivalent to that of dye (MB) molecules and therefore the diffusion of dye molecules to the core of those aggregates required higher thermal energy. Therefore with increase in temperature, increase in the adsorption capacity on dye removal was observed.

Figure 11. Effect of temperature on the adsorption capacity (Q_e) of PTh-Ni Composite. Conditions: initial concentration of MB= 600 mg/L; volume of MB solution= 10 mL; Contact time 60 min at 30, 40, 50, and 60°C; adsorbent dosage = 1.5 g/L; oscillator speed = 150 rpm; at neutral pH).

Thermodynamic parameters were evaluated to investigate the nature of the adsorption. The thermodynamic parameters including the Gibbs free energy ($\Delta G°$), enthalpy ($\Delta H°$), and entropy ($\Delta S°$) were calculated using the equations (11), (12) and (13) [37-38].

$$\Delta G = -RT \, In \, K_c \qquad --------- \quad (11)$$

$$In \, K_c = \frac{-\Delta H}{RT} + \frac{\Delta S}{R} \qquad --------- \quad (12)$$

$$K_c = \frac{Q_e}{C_e} \qquad --------- \quad (13)$$

where Q_e = equilibrium adsorption capacity (mgg^{-1}), C_e = equilibrium concentration (mgL^{-1}), $\Delta G°$= standard free energy change of adsorption, R= gas constant (8.314 J mol^{-1} K^{-1}), T= temperature (K). The negative $\Delta G°$ values at 30, 40, 50 and 60°C for the PTh-Ni composite are recorded in Table 4 which confirm the spontaneous nature and feasibility of the adsorption [39]. In addition, the decrease in the value of $\Delta G°$ with increase in temperature also suggests that the adsorption of MB on PTh-Ni composite is more favored at higher temperatures. The $\Delta H°$ value of PTh-Ni composite indicate the adsorption of MB is a physisorption process and the adsorption reaction is endothermic [34]. The standard entropy change ($\Delta S°$) was also observed to be positive (Table 4) which signifies an increase in randomness at the solid – solution interfaces.

Table 4. Thermodynamic parameters for the adsorption of MB onto PTh-Ni Composite.

Temperature (°C)	$\Delta G°$ (kj mol^{-1})	$\Delta H°$ (kj mol^{-1})	$\Delta S°$ (kj $mol^{-1}K^{-1}$)
30	-35.77	2.519	0.033
40	-38.48		
50	-41.70		
60	-46.67		

2.7. Desorption and repeatability studies

The cycles of adsorption–desorption process were successively conducted four times for each type of adsorbent. Desorption and repeatability studies were carried out in duplicate and their average adsorption capacities of each cycle are shown in Fig. 12, the MB adsorption capacity decreased after each cycle. This decrease is due to increase of MB-attached-adsorbent via chemical adsorption after each cycle, similar to that reported by Auta *et al* for Chitsan-clay composite [40-41].
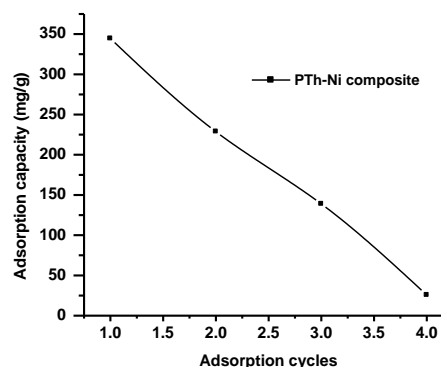
Figure 12. Repeatability of PTh-Ni composite adsorbent on adsorption capacity of MB. Conditions: adsorbent dosages = 1.5 g/L, [MB]= 600 mg/L, Contact time = 60 min, oscillator speed = 150 rpm.

2.8. Comparison with other studied adsorbents

The maximum adsorption capacity (Q_m) which was obtained from Langmur model (equation 8) for adsorption of MB onto the PTh-Ni composite were compared with various common adsorbents reported in Table 5.

Table 5. Values of adsorption capacity (Q_{max}) for the adsorption of MB on various adsorbents

Adsorbents	Q_{max} (mg/g)	Contact time	References
Clay	58.2	60 min	[42]
Hydrogel modified polysaccharide	48	90 min	[43]
Polythiophene – Sawdust Nano-Biocomposite	191	24 h	[3]
Polydopamine microspheres	90.7	60 min	[34]
M-MWCNTs	40.06	60 min	[44]
Graphene nanosheet (GNS)/ magnetite (Fe_3O_4)	43.82	60 min	[45]
Fe_3O_4@ PPy/RGO	270.3	60 min	[9]
PTh-Ni composite	384.61	60 min	This work

The easier synthesis, faster adsorption, higher adsorption capacity make the polythiophene and nickel composite more attractive as an adsorbents for MB removal from its aqueous solution.

2.9. Adsorption Mechanism

Dye molecule adsorption on the adsorbent may proceed through physical, chemical or combination of both at interfaces. Repeatability results indicate that a part of MB attached on to adsorbent via irreversible chemical adsorption. Moreover, as discussed in the effect of pH on MB adsorption, the electrostatic attraction is also responsible for the interaction of MB with adsorbents. The van der Waals interaction is also responsible for the adsorption of MB onto the polymers.

IV.CONCLUSION

1. Polythiophene nickel composite were electrochemically synthesized using thiophene, perchloric acid, nickel chloride in acetonitrile medium and used to be as high-efficient adsorbents for the removal of methylene blue dye from its aqueous solution. **2**. Weight of polymer aggregates decreased with increase in nickel chloride concentration.
3. Critical field intensity was observed at 3.6 V/cm beyond which weight of polymer aggregates decreased.

4. Electrical conductivity of PTh-Ni composite is found to depend upon nickel chloride concentration.
5. Fractal dimension (*D*) of growth patterns of PTh-Ni composite was calculated by box counting method and found in the range 1.7-1.8 in agreement with the value for Diffusion Limited Aggregation (DLA) model.
6. FT-IR spectra of PTh, PTh-Ni composite were compared, shifting is observed due to the interaction of Ni^{2+} with polythiophene.
7. TEM studies revealed the formation of PTh-Ni composite with an average diameter < 5 nm.
8. Further, we observed that the MB adsorption was highly dependent on initial MB concentration, contact time, pH and temperature.
9. In the kinetic studies, the pseudo-second-order kinetic model was demonstrated.
10. Adsorption of MB on polymer aggregates is found to be spontaneous, and endothermic in nature.
11. Polythiophene nickel composite belong to a new class of adsorbents for organic dye removal from polluted water.

V. ACKNOWLEDGEMENT

VI. REFERENCES

[1]. M. Shanehsaz, S. Seidi, Y. Ghorbani, S. M. R. Shoja and S. Rouhani, 2015, Polypyrrole- coated marnetic nanoparticles as an efficient adsorbent for RB19 synthetic textile dye: Removal and kinetic study, Spectrochimica Acta Part A: Molecular and Biomolecular Spectroscopy 149, 481-486.
[2]. L. Wang, J. Zhang and A. Wang, 2011, Fast removal of methylene blue from aqueous solution by adsorption onto chitosan-g-poly(acrylic acid)/attapulgite composite, Desalination. 266, 33-39.

[3]. R. Ansari, M. S. Tehrani and M. B. Keivani, 2013, Application of Polythiophene – Sawdust Nano – Biocomposite for Basic Dye Removal Using a Continuous System, Journal of Wood Chemistry and Technology 33, 19-32.

[4]. R. Jamal, L. Zhang, M. Wang, Q. Zhao and T. Abdiryim, 2016, Synthesis of poly (3,4-propylenedioxythiophene)/MnO2 composites and their applications in the adsorptive removal of methylene blue, Progress in Natural Science Materials International, 26, 32- 40.

[5]. X.G. Li, Z.Z. Hou, M. R. Huang and M. G. Moloney, 2009, Efficient Synthesis of Intrinsically Conducting Polypyrrole Nanoparticles Containing Hydroxy Sulfoaniline as Key Self-Stabilized Units. J. Phys. Chem. C, 113, 21586- 21595.

[6]. A S Abd- El- Aziz, 2006, New Jersey John wiley and sons.

[7]. W-Y Wong and P D Harvey, 2010, Recent Progress on the Photonic Properties of Conjugated Organometallic Polymers Built Upon the trans Bis(paraethynylbenzene)bis(phosphine)platinum(II) Chromophore and Related Derivatives. Macromol Rapid Commun, 31, 671-713.

[8]. A Rudge, J Davey, I Raistrick, S Gottesfeld and J P Ferraris, 1994, Conducting polymers as active materials in electrochemical capacitors. J. power sources, 47, 89 -107.

[9]. X. Peng, W. Zhang, L. Gai, H. Jiang, Y. Wang and L. Zhao, 2015, Dedoped Fe3O4/ PPy nanocomposite with high anti- interfering ability for effective separation of Ag (I) from mixed metal-ion solution, Chemical Engineering Journal 280, 197-205.

[10]. K. Shang, S. Ai, Q. Ma, T. Tang, H. Yin and H. Han, 2011, Effective photocatalytic disinfection of E .coli and S. aureus using polythiophene / MnO2 nanocomposite photocatalyst under solar light irradiation, Desalination, 278, 173-178.

[11]. .Y. Zhu, S. Xu and D. Yi, 2010, Photocatalytic degradation of Methyl orange using polythiophene/titanium dioxide composites, Reactive & Functional Polymers 70, 282-287.

[12]. H. Sert, Y. Yildiz, T. O. Okyay, B. Gezer, Z. Dasdelen, B. Sen and F. Sen, 2016, Monodisperse Mw- Pt NPs @ VC as Highly Efficient and Reusable Adsorbent for Methylene Blue Removal, J. Clust Sci 27, 1953-1962.

[13]. I. Das, R. Choudhary, S.K. Gupta and P. Agrawal, 2011, Nanostructured growth patterns and chaotic oscillations in potential during electropolymerization of aniline in the presence of surfactants, J. Phys. Chem. B. 115, 8724-8731.

[14]. R. P. Rastogi, I. Das, A. Pushkarna, A. Sharma, K. Jaiswal and S.Chand, 1992, Inexpensive laboratory experiments on crystal growth of water soluble substances in gel media, J. Chem. Educ. 69 (2) A47.

[15]. I. Das, N. R. Agrawal, S. K. Gupta and R. P. Rastogi, 2009, Fractal growth kinetics and electric potential oscillations during electropolymerization of pyrrole, J. Phys. Chem. A, 113, 5296-5301.

[16]. O. Pezoti Jr. , A. L. Cazetta, Isis P.A.F. Souza, K. C. Bedin, A. C. Martins, T. L. Silva and V. C. Almeida, 2014, Adsorption studies of methylene blue onto ZnCl2-activated carbon produced from buriti shells (Mauritia flexuosa L.) , Journal of Industrial and Engineering Chemistry, 20 (6), 4401–4407.

[17]. R. Ahmad and I. Hasan, 2017, Efficient Remediation of an Aquatic Environment Contaminated by Cr (VI) and 2,4- Dinitrophenol by XG-g-Polyaniline@ZnO Nanocomposite, Journal of Chemical & Engineering data DOI: 10.1021/acs.jced.6b00963.

[18]. I. Das, N.Goel, N.R. Agrawal and S.K. Gupta, 2010, Growth patterns of dendrimers and electric potential oscillations during electropolymerization of pyrrole using mono-and mixed surfactants , J. Phys. Chem. B. 114, 12888-12896.

[19]. A. K. Mishra, A. Sharma, I. Das and N. R. Agrawal, 2016, Electrochemical synthesis of dendritic nanosized conductive polythiophene cobalt composite as charge storage device, J. Indian Chem. Soc. 93, 971- 981.

[20]. M.J Jean. 2002, Frechet, PNAS, Dendrimers and supramolecular chemistry. (99), 4782- 4787.

[21]. Sherry Zhu and Timothy M. Swager, 1997, Conducting Polymetallorotaxanes: Metal Ion Mediated Enhancements in Conductivity and Charge Localization. J. Am. Chem. Soc, (119), 12568- 12577.

[22]. D. Gourier and G. Tourillon, 1986, Production of highly ordered organic conducting polymers (poly(3-methylthiophene)) under electrochemical inclusion of Cu/sup 2 +/ ions: an ESR study. J. Phys. Chem. (90), 5561- 5565.

[23]. J. Mardalen, E.J. Samuelsen, O.R. Gautun and P.H. Carlsen, 1992, X- ray scattering from oriented poly (3- alkylthiophenes), Synth. Met. 48, 363–380

[24]. Y.N. Li, G. Vamvounis and S. Holdcroft, 2002, Tuning Optical Properties and Enhancing Solid- State Emission of Poly(thiophene)s by Molecular Control: A postfunctionalization Approach, Macromolecules 35, 6900–6906.

[25]. B. Senthilkumar, P. Thenamirtham and R. Kalai Selvan, 2011, Structural and electrochemical properties of polythiophene, Applied Surface Science 257, 9063– 9067.

[26]. J. Coates, 2000, Interpretation of Infrared Spectra, A Practical Approach, Encyclopedia of Analytical Chemistry ,R.A. Meyers (Ed.), Chichester, 10815–10837, © John Wiley & Sons Ltd.

[27]. Y.H. Li, S.G. Wang, Z.K. Luan, J. Ding, C.L. Xu, and D.H. Wu, 2003, Adsorption of cadmium (II) from aqueous solution by surface oxidized carbon nanotubes, Carbon. 41, 1057- 1062.

[28]. L. Bai, Z. Li, Y. Zhang, T. Wang, R. Lu, W. Zhou, H. Gao, and S. Zhang, 2015, Synthesis of water – dispersible grapheme- modified polypyrrole nanocomposite and its ability to efficiently adsorb methylene blue from aqueous solution, Chem. Eng. J. 279, 757-766.

[29]. Y. Zhang, W. Wang, J. Zhang, P. Liu, and A. Wang, 2015, A comparative study about adsorption of natural palygorskite for methylene blue, Chem. Eng. J. 262, 390-398.

[30]. D. L. Zhao, G. D. Sheng, J. Hu, C. L. Chen, X. K. Wang, 2011, The adsorption of Pb (II) on Mg2Al layered double hydroxide, Chem. Eng. J. 171, 167- 174.

[31]. A. Aluigi, F.Rombaldoni,C.Tonetti, and L.Jannoke, 2014, Study of methylene Blue adsorption on keratin nanofibrous membranes, J.Hazard. Mater. 268, 156-165.

[32]. Z.Chen , J. Zhang, J. Fu, M. Wang, R. Han, and Q. Su, 2014, Adsorption of methylene blue on to poly(Cyclotriphoshazene- CO-4, 4' – sulphonyldiphenol) nanotubes: kinetics, isotherm and thermodynamics analysis, Hazard. Mater. 273, 263-271.

[33]. A. Mittal, R. Ahmad, and I. Hasan, 2016, Biosorption of Pb2+, Ni2+, and Cu2+ ions from aqueous solutions by L- cystein-modified montmorillonite- immobilized alginate nanocomposite, Desalination and Water Treatment, 57, 17790- 17807.

[34]. J.W. Fu, Z. H. Chen, M. H. Wang, S. J. Liu, J. H. Zhang, J. N. Zhang, R. P. Han, and Q. Xu, 2015, Adsorption of methylene blue by high- efficiency adsorbent (polydopamine microspheres): Kinetics, isotherm, thermodynamics and mechanism analysis, Chem. Eng. J. 259, 53-61.

[35]. Y. S. Ho, 2006, Second –order kinetic model for the sorption of cadmium onto tree fern: a comparison of linear and non linear methods, Water Res. 40, 119-125.

[36]. Y. Liu, Y. Y. Kang, B. Mu, and A. Q. Wang, 2014, Attapulgite/ bentonite interactions for methylene blue adsorption characteristics from aqueous solutions. Chem. Eng. J. 237, 403-410.

[37]. A. Khenifi, Z. Bouberka, F. Sekrane, M. Kameche, and Z. Derriche, 2007, Adsorption study of an industrial dye by an organic clay, Adsorption, 13, 149- 158.

[38]. A.S. Ozcan, B. Erdem, and A. Ozcan, 2004, Adsorption of Acid Blue 193 from aqueous solution onto Na- bentonite and DTMA- bentonite, J. Colloid Interface Sci., 280, 44- 54.

[39]. L. Ye, J.L. Fu, Z. Xu, R.S. Yuan, and Z.H. Li, 2014, Facile one-pot solvothermal method to nanocomposites with superior photocatalytic performance, ACS Appl. Mater. Interfaces 6, 3483-3490.

[40]. M. Auta, and B.H. Hameed, 2014, Chitosan- clay composite as highly effective and low cost adsorbent for batch and fixed-bed adsorption of methylene blue, Chem. Eng. J. 237, 352-361

[41]. L Wang, J. Zhang, and A. Wang, 2011, Fast removal of methylene blue from aqueous solution by adsorbtion onto chitosan-g-poly (acrylic acid)/ attapulgite composite, Desalination 266 (1-3), 33- 39.

[42]. A.Gurses, C.Dogar, M. Yalcin, M. Acikyildiz, R. Bayrak, and S. Karaca, 2006, The adsorption kinetics of the cationic dye, methylene blue, onto clay. J. Hazard. Mater. 131, 217-228.

[43]. A.T. Paulino, M.R. Guilherme, A.V. Reis, G.M. Campese, E.C. Muniz, and J. Nozaki. 2006, Removal of methylene blue dye from an aqueous media using superadsorbent hydrogel supported on modified polysaccharide, J. Colloid Interface Sci, 301, 55-62.

[44]. L. Ai, C. Zhang, F. Liao, Y. Wang, M. Li, L. Meng. And J. Jiang, 2009, Removal of methylene

blue from aqueous solution with magnetite loaded multi-wall carbon nanutube nanocomposite as adsorbent , J. Hazard. Mater. 164 (2-3), 1517-1522

[45]. L. Ai, C. Zhang, and Z. Chen, 2011, Removal of methylene blue from aqueous solution by a solvothermal- synthesized graphene/magnetite composite. J. Hazard Mater. 192 (3), 1515-1524.